

Visualizing Cell Structures with Minecraft

Tianyu Wu^{1,2,3,§}, Zane R. Thornburg^{4,5,§}, Kevin Tan^{3,4,6,§}, Seth Kenkel^{3,4},
Stephen A. Boppart^{3,4,5,6,7,8}, Rohit Bhargava^{2,3,4,5,6,7,9,10},
Zaida Luthey-Schulten^{1,2,3,4,5,*}

¹Center for Biophysics and Quantitative Biology, University of Illinois at Urbana–Champaign, Urbana, IL, USA

²Department of Chemistry, University of Illinois at Urbana–Champaign, Urbana, IL, USA

³National Science Foundation Science and Technology Center for Quantitative Cell Biology, Beckman Institute for Advanced Science and Technology, University of Illinois at Urbana–Champaign, Urbana, IL, USA

⁴Beckman Institute for Advanced Science and Technology, University of Illinois at Urbana–Champaign, Urbana, IL, USA

⁵Cancer Center at Illinois, University of Illinois at Urbana–Champaign, Urbana, IL, USA

⁶Department of Bioengineering, University of Illinois at Urbana–Champaign, Urbana, IL, USA

⁷Department of Electrical and Computer Engineering, University of Illinois at Urbana–Champaign, Urbana, IL, USA

⁸NIH/NIBIB Center for Label-free Imaging and Multiscale Biophotonics (CLIMB), University of Illinois at Urbana–Champaign, Urbana, IL, USA

⁹Department of Chemical and Biomolecular Engineering, University of Illinois at Urbana–Champaign, Urbana, IL, USA

¹⁰Department of Mechanical Science and Engineering, University of Illinois at Urbana–Champaign, Urbana, IL, USA

ABSTRACT Many microscopic images and simulations of cells give results in different kinds of formats, making it difficult for people lacking computational skills to visualize and interact with them. Minecraft—known for its three-dimensional, open-world, voxel-based environment—offers a unique solution by allowing the direct insertion of voxel-based cellular structures from light microscopy and simulations into its worlds without modification. This integration enables Minecraft players to explore the ultrastructure of cells in a highly immersive and interactive environment. Here, we demonstrate several workflows that can convert images and simulation results into Minecraft worlds. Using the workflows, students can easily import and interact with a variety of cellular content, including bacteria, yeast, and cancer cells. This approach not only opens new avenues for science education but also demonstrates the potential of combining scientific visualization with interactive gaming platforms for facilitating research and improving appreciation of cellular structure for a broad audience.

KEY WORDS cell visualization; Minecraft; computational biology; game-based learning

“*” corresponding author

“§” equal contribution

Received: 17 June 2024

Accepted: 8 November 2024

Published: 3 February 2025

© 2025 Biophysical Society.

I. INTRODUCTION

In recent years, the field of cellular biology has witnessed remarkable advancements in three-dimensional (3D) microscopic techniques, such as cryogenic soft x-ray tomography, cryogenic electron tomography (cryo-ET), and focused ion beam scanning electron microscopy,

enabling visualization of subcellular structures with resolution in nanometers (1–3). The results provide valuable spatial distributions of different organelles and proteins, which can further facilitate the development of more realistic 3D whole-cell models (WCMs) for research and educational purposes, enhancing our understanding of cellular functions and the complicated chemical reactions within cells.

The WCMs integrate all available structural and omics information to simulate the growth of the cell under certain conditions, which allows researchers and educators to explore the dynamic behavior of different macromolecules and even perform in-silico experiments (4, 5). Further, this technique not only illuminates the spatial organization and functional dynamics of cellular components but also facilitates the integration of complex biological concepts into public education through innovative methods. Among these, the use of game-based teaching methods, such as those used in Minecraft, has emerged as a particularly effective strategy for conveying complex scientific notions in an accessible and interactive manner (6).

Minecraft (version 1.21.06; Education Edition; Mojang Studios, Stockholm, Sweden) is a popular 3D sandbox game that offers players freedom to construct and observe complex structures made of blocks (7). By leveraging this platform, we have developed a generalized workflow for integrating 3D whole-cell structures, obtained through experimental techniques or WCM simulation into the Minecraft world. This innovative approach enables individuals to immerse themselves into the cell, navigate through the cytoplasmic membrane, observe the spatial distribution of organelles, and gain a tangible understanding of relative sizes and quantities.

Here, we provide three illustrative examples to demonstrate the versatility and effectiveness of our approach. First, we detail the process of extracting the structural simulated WCM data of *Saccharomyces cerevisiae* (baker's yeast) and the minimal bacterium JCVI-syn3A from cryo-ET images, subsequently reconstructing their whole-cell geometries within the Minecraft world (5, 8).

Then we explore the imaging of cancerous and normal breast cells by using holotomography to highlight structural differences by visualizing the cells in Minecraft (9). Furthermore, the visualization of small metabolite molecules is achieved through label-free atomic force microscopy–based infrared (AFM-IR) spectroscopy, offering insights into cellular metabolism without the need for intrusive labeling techniques (10). The workflow involves extracting the cell structures and postprocessing, which may help students better understand modern microscopy techniques.

By merging the analytical capabilities of various imaging systems with the interactive and immersive environment of Minecraft, our approach not only facilitates a novel educational tool for illustrating biological concepts but also represents a significant step forward in the digital visualization of cellular structures. This synergy between cutting-edge scientific techniques and accessible digital platforms holds the potential to revolutionize biological research and game-based education, bridging the gap between complex scientific knowledge and public understanding.

II. SCIENTIFIC AND PEDAGOGICAL BACKGROUND

A. Pedagogic background

Our approach is a multilevel design for one platform in which we bolster the understanding of subcellular structures among students and other interested parties through a comprehensive educational strategy that includes three main components: data acquisition and postprocessing, integration into Minecraft, and interactive exploration. The comprehensive, yet flexible, design of our approach permits the selection of specific workflows that can be customized to fit the learning objectives and the proficiency level of the target audience (Figs 2, 3, 4; Table 1).

For elementary school students, the primary objective should be fostering an interest in biological sciences and coding. Consequently, it is advisable to omit the stages of data acquisition and postprocessing. The emphasis should be placed on introducing simple biological concepts

Table 1. Suggested workflow activities based on education level.

| Examples (related workflow figure) | Stages (related figure) | Elementary school | Middle and high school | College | Public |
|--|---------------------------|-------------------|------------------------|---------|--------|
| Yeast with cryo-electron tomography (Figure 2) | Segmentation (Fig 2A) | | | ✓ | |
| | Reconstruction (Fig 2B,C) | | | ✓ | |
| | Integration (Fig 2D,E) | | ✓ | ✓ | |
| | Exploration (Fig 2F) | ✓ | ✓ | ✓ | ✓ |
| Minimum cell with whole-cell methods (Figure 3) | Segmentation (Fig 3A) | | | ✓ | |
| | Reconstruction (Fig 3B–E) | | | ✓ | |
| | Integration (Fig 3F) | | ✓ | ✓ | |
| | Exploration (Fig 3F) | ✓ | ✓ | ✓ | ✓ |
| Human breast cell with holotomography (Figure 4) | Segmentation (Fig 4C) | | | ✓ | |
| | Integration (Fig 4D) | | ✓ | ✓ | |
| | Exploration (Fig 4D) | ✓ | ✓ | ✓ | ✓ |

to enhance their understanding of basic biological facts.

At secondary (high school) and tertiary (collegiate) education levels, where the study of cell biology is more concentrated, the focus should be on engaging students with interactive visualization workflows that are complemented with explanations of the functions of various organelles, such as the nucleus and mitochondria. The curriculum can be broadened to incorporate data-processing techniques. This expansion is crucial for clarifying the process of capturing ultrastructural images through advanced imaging techniques such as cryo-ET and holotomography.

For students motivated by autonomous exploration of subcellular characteristics, the curriculum offers data acquisition and segmentation methods. These techniques guide students through the process of handling raw data that can be downloaded from various open-source databases. Students are then introduced to the use of statistical methods in Python (version 3.12; Python Software Foundation, Wilmington, Delaware, USA) for analyzing structural aspects of organelles, such as volume, surface area, and the surface area-to-volume ratio. With a comprehensive dataset, students can explore the interactions between different cellular components (e.g., the endoplasmic reticulum, plasma membrane) and conduct comparative studies of various eukaryotic cells, shedding

light on the unique features of each type of organelle.

This educational framework is particularly effective for differentiating between bacterium minimum cell and eukaryotic cell yeast, as well as between pathological (cancerous) and healthy cells. It allows educators to demonstrate the absence of organelles in bacteria cells and the nonexistence of a nuclear membrane, and health care professionals can use it to explain the nature of precancerous lesions and the mechanisms of action of therapeutic interventions (e.g., chemotherapy).

B. Minimal cells

With the goal of creating a cell with the fewest genes necessary to live, JCVI-syn3A was synthesized by genetically reducing the gram-positive bacteria *Mycoplasma mycoides subsp. capri* strain GM12. Genes that were determined to be nonessential were removed from the genome iteratively until the genome had been reduced from ~1,000 genes to 493 genes, of which 452 codes were for proteins (11). The 493 genes in Syn3A are coded on a single 543-kbp circular chromosome; for comparison, the genome of *Escherichia coli* comprises more than 4,600 genes (11). Syn3A is ~400–500 nm in diameter and doubles in roughly 2 h. Because of its simplicity, Syn3A has now been used as a platform for constructing WCMs with the goal of evolving complete cell states forward in

time to probe time-dependent cell behavior and predict how perturbations will affect the cell state (5). Through these models and other experimental characterization, progress is being made in understanding the physical and chemical principles of life.

C. Baker's yeast

Baker's yeast is a favorite organism in genetics and cell biology research (12). Despite yeast being relatively simple, eukaryotic, single-cell micro-organisms, numerous studies have demonstrated that many cellular biological mechanisms are remarkably preserved across species, from yeast to mammals (13). Baker's yeast contains all the defining subcellular structures of eukaryotes, including a well-defined nucleus, endoplasmic reticulum, mitochondria, Golgi apparatus, and complex cytoskeletal elements. Its accessibility and the ease with which it can be manipulated genetically make it an exemplary model for studying cellular processes such as DNA replication, transcription and translation, cell division, and metabolism. Because of its instrumental role in the fermentation process and as a staple in genetic research, it has become a familiar entity not only within the scientific community but also to the general public.

D. Breast cancer cells

In 2020, excluding nonmelanoma skin cancer, breast cancer was the most commonly diagnosed cancer for women in the United States and was second only to lung cancer in number of deaths caused (14). The study of breast cancer has remained at the forefront of cancer research for decades, and our understanding is ever growing. Currently, the most common method for breast cancer diagnosis is two-dimensional (2D) histopathology. Histopathologists are trained to analyze features such as the size of the cell nucleus to determine the cancer grade. Although this is customary practice, 2D histopathology is inherently an incomplete view of the 3D tissue, and the processing needed to slice and stain histology can cause misleading distortions. Therefore, a complete 3D picture may lead to development

of better diagnosis and treatment. For example, in human breast epithelial cells, the number and spatial distribution of nucleoli correlates with the cancer grade, which is explained by the increased transcription in these cells (15). It is critical that an understanding of the 3D changes that take place during cancer are made accessible to increase public awareness and interest in novel directions in cancer research.

We adapted the cell culture model used in (15) to compare normal and abnormal human breast epithelial cells. The three cell lines included the normal cell line hTERT-HME1, the metastatic adenocarcinoma cell line MDA-MB-231, and the fibrocystic disease cell line MCF10A. The three cell lines are immortalized; however, hTERT-HME1 and MCF10A cells are not tumorigenic. The MCF10A cell line originates from proliferative benign breast tissue. One of the most appealing physical characteristics of this cell line is that it forms spheroid structures when cultured in a 3D matrix (16). The ability to grow 3D cell clusters provides a system that is more realistic than a 2D cell culture on a substrate and is useful when trying to characterize properties such as cell–cell interactions. We use this cell line as a representative for AFM-IR spectroscopy images.

E. Cryo-ET

Cryo-ET has emerged as a technique in the field of structural biology, particularly for investigating the ultrastructure of eukaryotic cells at 2–5-nm resolution. This method operates by capturing a series of 2D images at various tilt angles, ranging up to $\pm 70^\circ$, by using a transmission electron microscope (17). Each image in the series, known as a tilt series, provides a different perspective of the specimen. These images are meticulously aligned and subsequently used in a process called “back projection” to assemble a 3D reconstruction, or tomogram, of the specimen.

This approach allows researchers to visualize biological structures in their native environment to a resolution of $\sim 2\text{--}8$ nm from all three dimensions without the distortions or losses typically associated with traditional sectioning methods. This advanced imaging method allows scientists

to observe cell structures in their original state, preserved rapidly frozen in time, without the need for dyes or fixatives that can alter the cellular architecture (18). Consequently, cryo-ET is a powerful tool for elucidating the fundamental mechanisms of cellular processes and the architectural principles of cellular organization.

F. Holotomography

Digital holographic microscopy is a form of optical microscopy in which, instead of capturing a projected image, a hologram of the object's light wave front is digitally recorded and reconstructed into an image by using a computer algorithm. This technique, which leverages interference with a reference wavefront to capture amplitude and phase information, provides a more comprehensive view of the object compared with traditional microscopy, which records only intensity (19). The phase image allows for estimation of the refractive index (RI) of thin, transparent samples and provides a quantitative label-free contrast.

An extension of digital holographic microscopy measures high-resolution 3D holographic images and is a type of digital holographic tomography commonly referred to as “holotomography” (9). The technique illuminates the sample at numerous oblique angles, which forms holograms containing higher spatial frequencies present in the sample, increasing the resolution beyond the diffraction limit of the microscope. Next, a 3D RI image is computed from these holograms by sequentially changing the focal distance parameter and applying a physics-based digital reconstruction. This technique, described in detail in (9), has been commercialized by Nanolive (Nanolive SA, Tolochenaz, Switzerland), which sells holotomography devices designed for quantitative-phase imaging of 3D features in cell culture.

III. MATERIALS AND METHODS

The methodology of this study is structured into a workflow aimed at transforming computational models and experimental imaging into an interactive 3D model within the Minecraft game environment, thus facilitating an immersive

exploration of cellular structures for educational purposes. We have organized a GitHub repository so that users of each education level can access files of interest (e.g., users who want to download and explore the Minecraft worlds, users who want to see examples of code used to generate the structures in Minecraft) (20). The general workflow includes several phases.

An initial step, data acquisition, involves collecting detailed imaging data of cellular structures. Advanced microscopy techniques, including cryo-ET, holotomography, and AFM-IR spectroscopy, capture the details at subcellular levels. After data acquisition, segmentation occurs; specialized software is used to segment different subcellular structures within the raw imaging data. This process requires expertise in computational image analysis to accurately delineate organelles and other cellular components. Professional tools are used to ensure that the segmentation is precise, capturing the nuanced geometries and spatial relationships critical for constructing reliable models (Resources folder in [20]).

Upon acquiring computational structures or segmented imaging data, we proceed to the reconstruction phase, in which raw data are further processed and converted into file formats supported by a SchemGen graphical user interface (GUI) (SchemGen_GUI; .npy, .tiff). This step involves a series of procedures, including extrapolation and transformation of coordinates. The results are 3D separate binary masks of each organelle or subcellular structure ready for integration into Minecraft (Resources folder in [20]).

The next phase involves integrating the reconstructed 3D models into the Minecraft game environment, which requires the conversion of 3D data into Minecraft-compatible schematics. These can be generated by using either SchemGen_GUI or scripts written by experienced users. We then used Amulet Map Editor (version 0.10.27; Amulet Team) to load these schematic files into Minecraft worlds (Schematics and SchemGen_GUI folders in [20]).

After the schematic files have been integrated into a Minecraft world, the exploration phase includes the cell structure being explored in Minecraft. This step requires only moving the

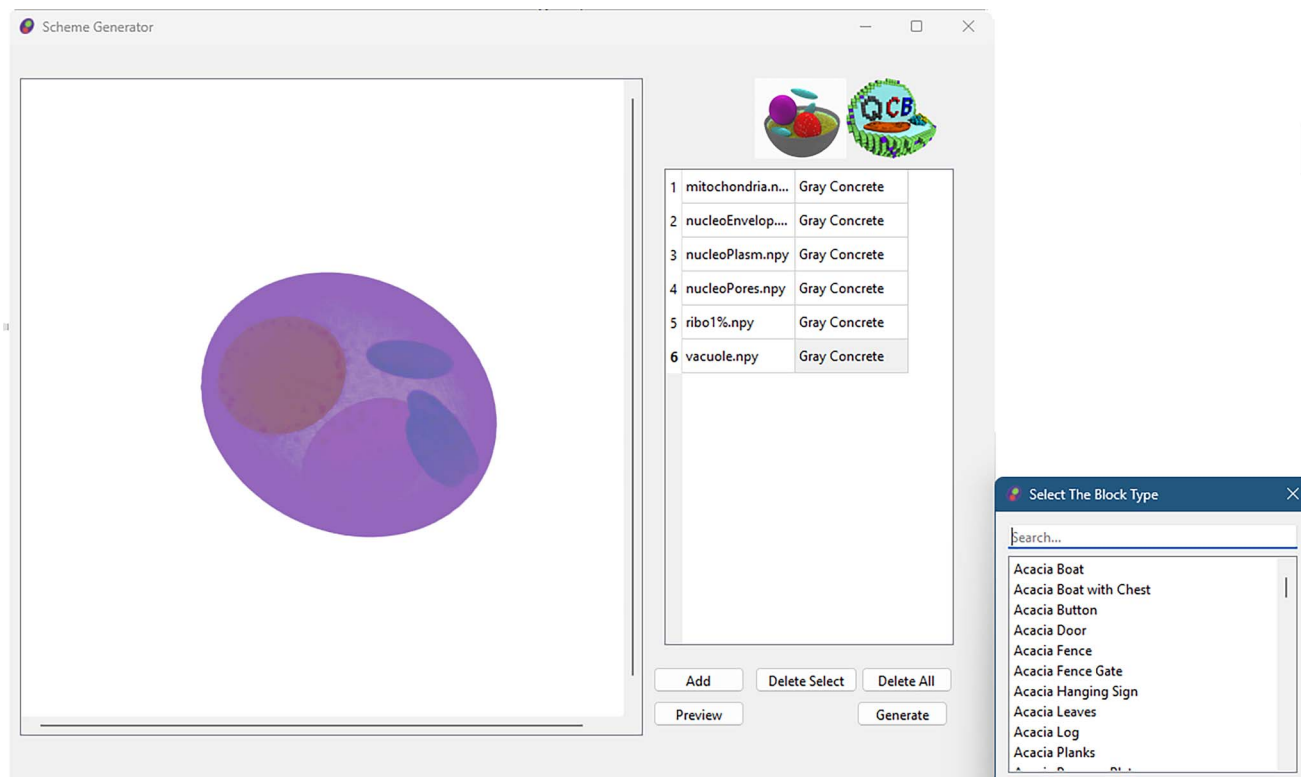


Fig 1. Graphical user interface showcasing a schematic file of baker's yeast. Left window: preview of the structure in the left panel, alongside a list of imported .npy files representing different subcellular structures. Right window: selectable list of block types for user interaction.

downloaded World folder into the Minecraft world Saves folder on a computer installed with Minecraft. Then the Minecraft world can be opened to explore the cells. For users who want to explore the worlds, these World folders are provided as zip files (Worlds folder in [20]).

In the subsequent subsections, we describe the exact workflows for four systems. The first and second workflows use data from cryo-ET and WCMs to elucidate the differences between eukaryotic yeast cells and the minimal bacterial cell JCVI-syn3A. The third workflow focuses on distinguishing between cancerous and noncancerous human breast cells, highlighting the structural alterations induced by cancer. Finally, the last workflow uses 2D images obtained from AFM-IR spectroscopy to visualize metabolic molecules in the human epithelial cell line MCF10A.

A. Importing structures into Minecraft

To facilitate the user visualizing and integrating the biological structures into the virtual environment with ease, we designed a GUI by

using the Python (version 3.12; Python Software Foundation, Wilmington, Delaware, USA) packages mcschematic and PyQT6, which are available in the SchemGen_GUI folder in (20). This interface was developed to integrate segmented biological data into the world of Minecraft for educational and research uses (Fig 1).

First, in the beginning of this process, one would include .npy files produced at the former stages of segmentation; after that, the user would be required to label the specific Minecraft block types per each biological structure as an aid for the visual separation between those structures. This can be performed by double-clicking the name of the corresponding .npy file in the GUI and then choosing a name from the predefined list of blocks. Without user selection, the default gray concrete is chosen, which is probably not a good choice for the differentiation of structures. For block types, we propose that stained glass blocks represent membranes and cell walls, and the use of concrete blocks is recommended to be used for other organelles in a manner that makes visual interpretation more straightforward.

The GUI preview allows the user to get an idea of the spatial distribution of the structures before importing into the Minecraft world. A schematic file was produced, and in the Amulet World Editor, the schematic file was implemented on a Minecraft world. Amulet is the latest editor of its kind and is used to create custom worlds for the Minecraft world. It is designed for precise placement, rotation, and scaling of these biological structures within a chosen virtual landscape. For convenience purposes and to make the transition into free, independent learning smoother, we offer two predesigned worlds, which can be found in the void and in a single block-thick bedrock layer in (20).

After the schematic file has been successfully integrated with Amulet, the last step is to place the World folder into the Minecraft saves directory, which is located in different places based on the operating system or Minecraft version used. Users may need to refer to resources indicating the location of the Minecraft Saves folder on their computer. An example of how to download the Minimal Cell Minecraft world from the Worlds folder in (20) is demonstrated in Video S1.

Loading a structure requires experimental or computational data annotated in 3D. Here, we describe the scientific efforts to generate cell structures for baker's yeast, a minimal bacterium, and human epithelial cells. Each of the workflows involves a different set of experimental and computational techniques to obtain their respective cell structure.

B. Cryo-ET workflow with baker's yeast

We first explore the sources and types of data essential for reconstructing 3D models from 2D images, specifically focusing on open-source electron microscopy/tomography datasets. Among the notable repositories are the Electron Microscopy Public Image Archive, the Electron Microscope Data Bank, and Open Organelle (21–23). These databases typically host two categories of data: raw data, which are unprocessed and require reconstruction, and processed data.

Our practical example uses processed data obtained from a study on baker's yeast cells (8). These cells were cultured, prepared, and imaged by using cryo-ET, yielding detailed structural information. The tomographic reconstructions were processed by using software packages IMOD (version 4.11; Boulder Laboratory for 3-D Electron Microscopy of Cells, University of Colorado, Boulder, Colorado, USA), which is a commonly used tool for reconstructing these images into a 3D density map for initial reconstruction, and EMAN2 (version 2.99; National Center for Macromolecular Imaging, Baylor College of Medicine, Houston, Texas, USA) for subtomogram averaging (24, 25). Segmentation of the tomograms to identify individual organelles was achieved by using nonlinear anisotropic diffusion filtering and automatic segmentation tools such as TomoSegMemTV, with further processing in Amira (version 6.4; Thermo Fisher Scientific, Waltham, Massachusetts, USA) by Thermo-Fisher (26).

The next stage involves converting the segmented tomographic data into a format suitable for 3D modeling and visualization within Minecraft. Postprocessing results in the generation of .npy files, which contain binary 3D matrices representing the different segmented structures (27). The workflow for integrating this data into Minecraft starts with importing the .npy files corresponding to various organelles or sub-cellular structures. By using the geometric characteristics of each structure, different extrapolation methods are selected for reconstruction.

With the use of the yeast data as an example, (Figure 2) the process begins with identifying the nucleus structure and density of nuclear pores from the respective .npy file. A custom loss function, along with the `scipy.optimize` package, is used to calculate the centroids, radii, and orientations of the nucleus (28). This procedure is replicated for other structures such as the plasma membrane and mitochondria. For structures such as the cell wall, for which direct data may not be available, estimations based on the volume ratio are used to adjust the parameters derived from the plasma membrane.

By using an empty lattice generated by Region-Builder in Lattice Microbes (+ Lattice Microbe, version 2.5; Zaida Luthey-Schulten Group, University of Illinois, Urbana-Champaign, Urbana, Illinois, USA) as a foundational framework, the primary method for building a comprehensive 3D model of yeast involves fitting ellipsoids to represent key cellular structures (e.g., nucleus envelope, plasma membrane, mitochondria, vacuole), leveraging either custom functions or equivalent ones from existing libraries, such as RegionBuilder.ellipsoid (8). This ellipsoid-based strategy is central to reconstructing the yeast's complex anatomy from sliced data to a holistic model, which enables detailed investigation into its structural characteristics, including nuclear pore density and surface area. Endoplasmic reticulum and Golgi apparatus cannot be rebuilt, because they are not ellipsoid-like organelles. Additionally, the model supports detailed positioning of nuclear pores along the nuclear envelope and strategic placement of ribosomes throughout the cellular space, facilitating simulations of ribosomal distribution that can range from uniform to variable densities, guided by user-defined parameters.

C. Lattice microbe workflow with minimal cells

The structure of the genetically minimal cell JCVI-syn3A comes directly from a published whole-cell simulation (5). Construction of the cell's architecture started with ribosome positions from cryo-ET of Syn3A, where template matching was used to map electron density to a ribosome structure from related bacteria (PDB:5MDZ). A full discussion of the process of this template-matching process was published in (29). The ribosomes annotated in the cryo-ETs were used as obstacles in determining structures of the circular chromosome by using a lattice polymer model, in which each monomer (in this case, Minecraft block) has edge lengths of 4 nm, representing roughly 12 bp of DNA. The lattice polymer model was also influenced by experimental chromosome contact maps, specifically chromosome conformation capture, revealing that Syn3A's chromosome is

generally relaxed and lacks significant persistent interaction domains and supercoiling.

The Syn3A structure presented here uses a single chromosome configuration simulated by using the lattice polymer model; the exact procedures for these simulations are thoroughly described in (29). The ribosome positions and chromosome configuration were then imposed onto an 8-nm cubic lattice for the purpose of the whole-cell simulation. Finally, a membrane with a radius of 200 nm was generated on the same cubic lattice to confine the cytoplasm. These whole-cell simulations included chemical reactions to express all 493 genes in Syn3A, as well as its metabolic network. The particles representing other macromolecules (e.g., proteins and mRNA) have not been included in the Minecraft structure here, so the cytoplasm is empty for players to explore the chromosome and ribosomes.

More extensive discussion of the Syn3A model and a comprehensive workflow to generate the cell structure can be found in Figure 2 in (5). Similar to the yeast model, we can import the subcellular structures into a Minecraft representation; the workflow follows Figure 3C–F. For Syn3A, we have incorporated only structures of the membrane, DNA, and ribosomes. To prevent coarse-graining of the DNA representation (4-nm cubes) and to make the cytoplasm less crowded relative to the size of the player, the entire structure was constructed with 4-nm Minecraft blocks.

D. Holotomography workflow with breast cancer cells

The MDA-MB-231 human breast cancer cells and hTERT-HME1 normal human breast cells were obtained from American Type Culture Collection. The MDA-MB-231 cells were maintained in phenol red-free growth medium comprising Dulbecco's Modified Eagle Medium (Thermo Fisher Scientific, Waltham, Massachusetts, USA) supplemented with 10% fetal bovine serum (Cytiva Life Sciences, Marlborough, Massachusetts, USA) and 1% penicillin-streptomycin (Thermo Fisher Scientific, Waltham, Massachusetts, USA). The hTERT-HME1 cells were grown by using the Mammary Epithelial Cell

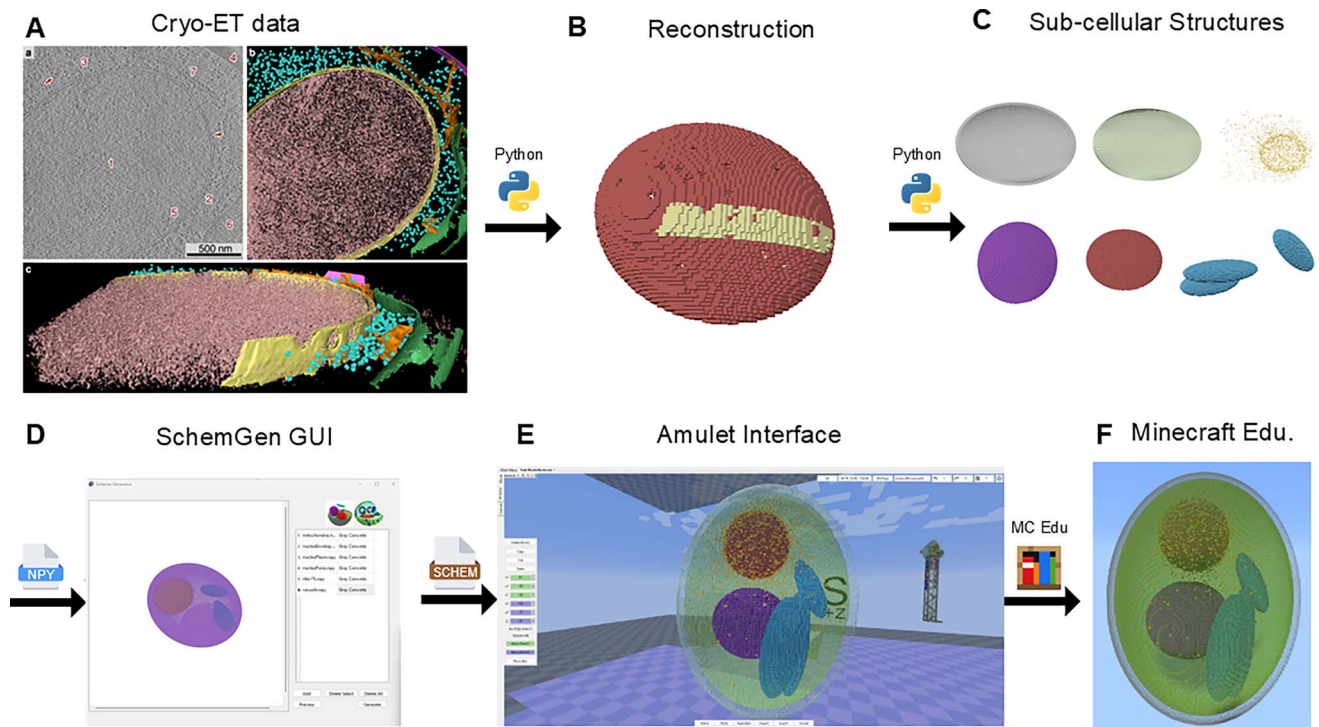


Fig 2. Workflow demonstration of importing baker's yeast from cryo-ET data. (A) Top left: raw data acquired from cryo-ET; top right and bottom: 240 nm slices of baker's yeast after segmentation. Reprinted with permission from (8). © 2017 American Chemical Society. Nuclear envelope, yellow; ribosomes, cyan; cell wall, magenta; mitochondrion, green; endoplasmic reticulum, orange. (B) Extrapolation of the nucleus envelope. Original data, yellow; extrapolation, red. (C) Visualization of separate .npy files with subcellular structures. Top left to bottom right: cell wall, gray; cell membrane, lime green; ribosomes, yellow; vacuole, purple; nucleus envelope, red; mitochondria, blue. (D) Graphical user interface to integrate all .npy files into a schematic file. (E) Amulet Editor imports a schematic file into a Minecraft world; same color scheme as (C). (F) Final results displayed in Minecraft Educational Edition; same color scheme as (C).

Growth Medium Bullet Kit (Lonza CC-3150; Lonza Group AG, Basel, Switzerland), which was prepared as recommended by the American Type Culture Collection. The cell lines were grown in a 95% relative humidity atmosphere with 5% CO₂ at 37°C. Cells were passaged by using 0.25% trypsin-EDTA solution (Thermo Fisher Scientific, Waltham, Massachusetts, USA) to detach the cells from the surface of the flask after reaching ~80% confluence and seeded into 35-mm glass-bottom imaging dishes (Ibidi 81218-200; Ibidi, GmbH; Fitchburg, Wisconsin, USA) with 1 mL of growth medium. Cells were allowed to adhere overnight before imaging with holotomography (3D Cell Explorer-fluo, NanoLive SA, Switzerland).

The 3D Cell Explorer-fluo was outfitted with a stage-top incubator (UNO-T-H-CO₂, OkoLab S.R.L, Italy), which maintained the cells during imaging in the same atmosphere and temperature in which they were cultured. Imaging

dishes containing the human breast cells were quickly moved from the cell culture incubator into the stage-top incubator for imaging. Holotomographic data were acquired by using the microscope's software, which allows for both single acquisition and automated time-series imaging for up to 96 h. The 3D Cell Explorer-fluo uses a class 1520 nm laser to illuminate the sample with very low intensity (0.2 mW/mm²), enabling long-term imaging with low phototoxicity. The microscope software uses hardware-accelerated processing to convert raw holographic data into 3D RI images that are visualized in real time and can be exported for external analysis. The optical (Rayleigh) resolution of the 3D Cell Explorer-fluo is ~190 nm in the lateral directions and 400 nm axially. Although this resolution is high enough to resolve larger subcellular structures such as the nucleus and mitochondria, it cannot resolve small structures such as individual

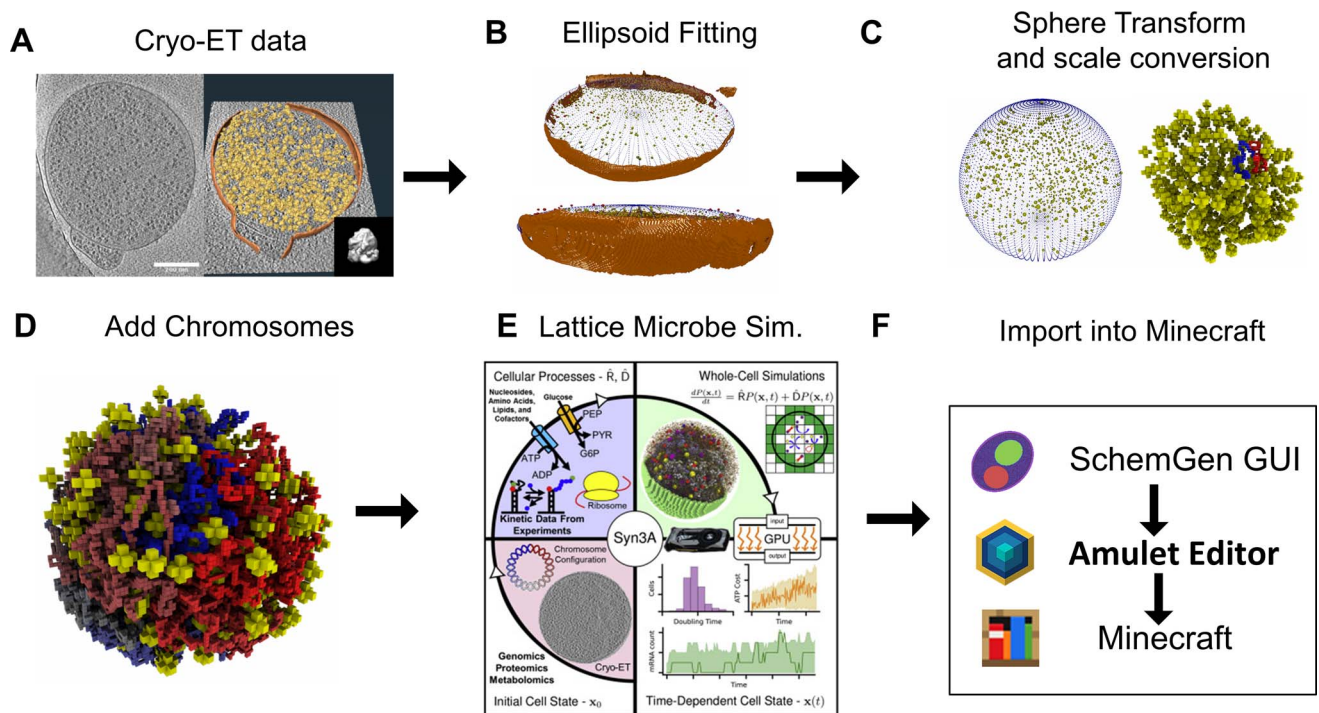


Fig 3. Workflow demonstration of minimal bacterial cell syn3A. (A) Left: single z-slice of the tomographic reconstruction; right: ribosomes (yellow) identified by using template matching and membrane segmentation (orange) superimposed on the z-slice. (B) Fitting the blotted cell shape (orange) around ribosomes with minimal surface area enclosing ellipsoids method. (C) Transformed to its natural spherical morphology and converted to 8 nm per cube representation. (D) Circular and self-avoiding chromosomes are generated as a lattice polymer around ribosomes. (E) Lattice microbe simulation (Sim.) to evolve the minimal bacterial system. (F) Export the structure as a .npy file and implement into Minecraft with the same procedure as for yeast. (A)–(D) reprinted from (28) with permission; (E) reprinted from (5) with permission.

ribosomes. The microscope has a field of view of $90 \times 90 \times 30 \mu\text{m}^3$. The image is sampled close to the optical resolution, and the voxel size in the reconstructed 3D volume is approximately $200 \times 200 \times 366 \text{ nm}^3$. After imaging the breast cancer cells, .tiff z-stacks containing RI values were exported.

The RI images of the breast cells were segmented into components by using ImageJ (Fiji, version 2.14.0; Eliceiri lab at the University of Wisconsin Madison, Madison, Wisconsin, USA) (30). To make this process faster and more reproducible, each step was recorded and compiled into a Jupyter notebook that accesses ImageJ through Python by using PyImageJ (31). The Jupyter notebook is available through the Resources folder in (20). The image was first cropped of edge artefacts, then resampled in the axial direction, resulting in approximately isotropic voxels $200 \times 200 \times 200 \text{ nm}^3$ in dimension. The contrast was then enhanced, and the background was subtracted. Next, the cytoplasm of the cells

was segmented by applying a median filter, followed by automatic thresholding by using the method proposed in (32). A 3D morphological closing operation from (33) was used to remove holes.

By using this division of the cytoplasm, a segmentation of the cell membrane was generated by subtracting the result of a 1-pixel radius 3D erosion of the cytoplasm from itself. We then segmented the organelles with higher RI than the cytosol such as mitochondria. The iterative thresholding algorithm from the 3D ImageJ Suite was used, followed by 3D dilation (34). The membrane of the organelles was found in the same manner as the membrane for the cell. Finally, the nucleus and nucleoli were manually segmented by using the Segmentation Editor in ImageJ. The results of each segmentation described here were saved as binary images, in which locations of the subcellular structures are set to 255 and everywhere else is set to 0. The second section of the Jupyter

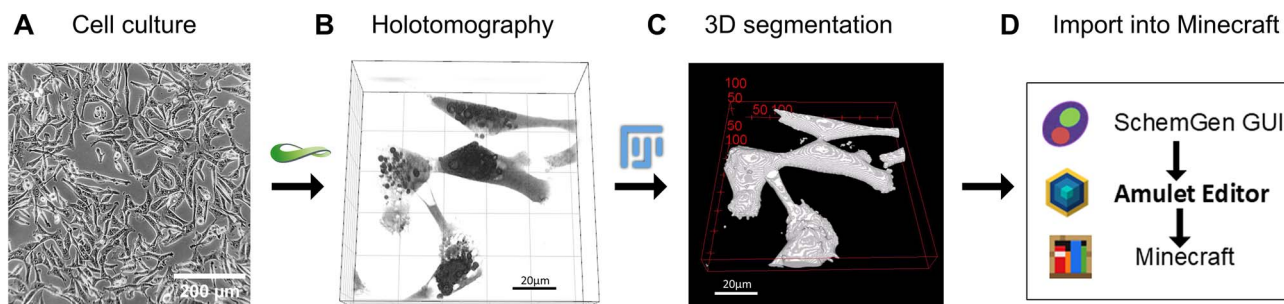


Fig 4. Workflow of creating Minecraft models from holotomographic images of cultured breast cancer cells. (A) Human epithelial breast cells: MDA-MB-231 (cancer) and hTERT-HME1 (normal) were grown in culture. (B) Holotomographic images were acquired, yielding raw refractive index values at each voxel. (C) Identifiable cell features in the images were segmented by using both automatic and manual tools provided by ImageJ. (D) TIFF files containing each segmented feature are converted to a unique Minecraft block to be loaded into Minecraft by using Amulet Editor.

notebook reads each file that contains a subcellular structure of interest and converts the voxels to a unique block type in a schematic file. The schematic file is loaded into Minecraft by using the Amulet Editor.

E. Label-free AFM-IR spectroscopy imaging workflow

The image collected by using the AFM-IR spectroscopy image comes directly from Figure 5 in (10). In AFM-IR spectroscopy, the IR spectrum of the sample at each pixel is collected by measuring the IR-induced expansion of the sample caused by an incident IR light source. This design enables label-free spatial mapping of chemical composition. Some methods measure the magnitude of the cantilever deflection, but the resolution of the image presented here was achieved by mounting the sample to a piezo actuator to maintain zero (or null) deflection. With this null-deflection AFM-IR (NDIR) method, the IR spectra can instead be collected by measuring the applied piezo voltage to maintain zero deflection. Extensive discussion of the theory and instrument development for this method, cell culturing procedures, and sample preparation can be found in (10). The cells imaged by using NDIR are MCF10A cells, a human mammary epithelial cell line. To produce the image, the IR intensities of three signals were combined to form the RGB channels: 990 cm^{-1} (red), $1,550\text{ cm}^{-1}$ (green), and $1,660\text{ cm}^{-1}$ (blue). The original NDIR image is 988×988 pixels with a resolution of $30 \times 30\text{ nm}$ pixels (or a $30 \times 30\text{ }\mu\text{m}$ field of view).

To fit the entire label-free IR image into one field of view in Minecraft, we reduced the size of the original image. ImageJ was used to reduce the size of the original image from 988×988 to 247×247 pixels. Additionally, we found that the bit depth of the image needed to be reduced because of color conversion into the Minecraft representation. Unfortunately, the number of colors that can be represented by Minecraft blocks is limited without user modifications to the source code of the game itself. For example, 16 main colors can be used for concrete, stained glass, and wool block types. Although some other block types can be used to gain access to more colors—for example, a user could use a sand block to represent a tan color block—we still do not have access to a full RGB color scale. A greater bit depth for color in the original image resulted in the color conversion to Minecraft creating artificial color variations in the image. We found that exporting the image to 8-bit color format from ImageJ greatly reduced the number of artefacts created by the color conversion. To generate a structure that incorporates a broader range of color, we generated the schematic by using a web tool that has mapped more Minecraft blocks to the RGB color scale. An example resource can be found in the Resources folder in (20).

IV. RESULTS

A. Minimal cell and baker's yeast

The structural details of baker's yeast are illustrated in Figure 5A, and a demonstration of

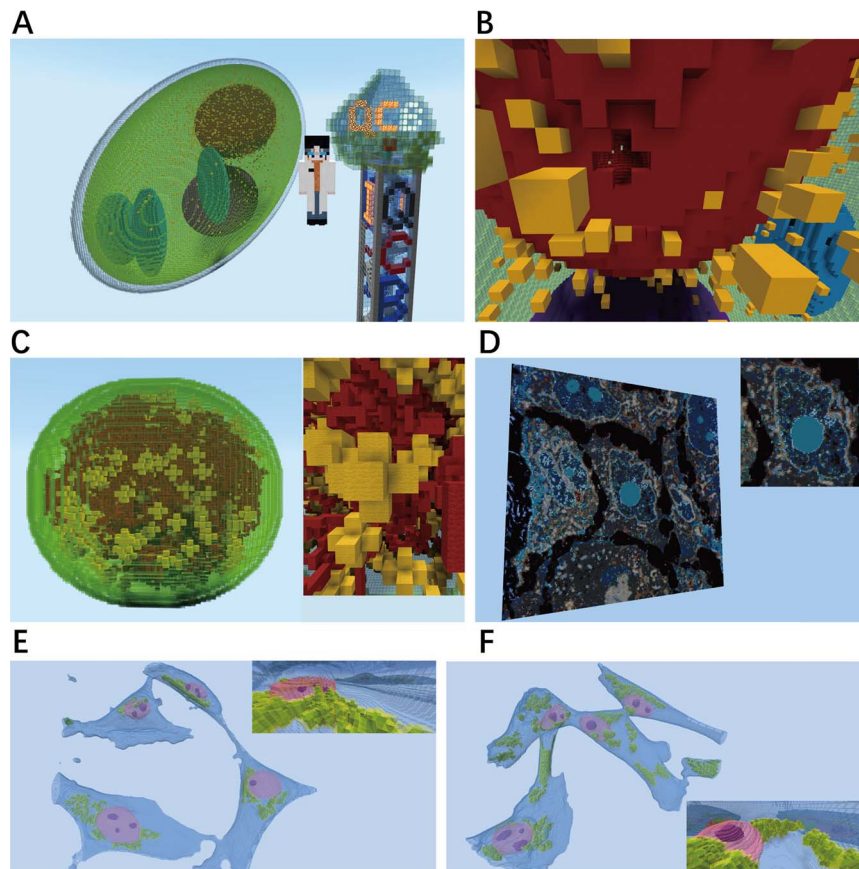


Fig 5. Results of examples in Minecraft. (A) Baker's yeast and University of Illinois Tower with QCB (Quantitative Cell Biology) logo. A video exploring the yeast structure is shown in Video S2. The structure shows the cell wall depicted by using stained glass, the cell membrane in lime green, mitochondria in blue concrete, the vacuole in purple concrete, the nucleus in red concrete, and ribosomes in yellow concrete; notably, nuclear pores are visible upon closer examination of the nucleus. (B) Nuclear pore in the baker's yeast as a hollow cross region embedded in the red nuclear envelope; scale: 28 nm/block. The cell membrane is illustrated in lime green—stained glass, 500 ribosomes are shown in yellow concrete, and DNA is represented in red concrete. (C) Minimal bacterial cell JCVI-syn3A. Right: interior structure; yellow: ribosomes; red: DNA; scale: 4 nm/block. (D) Metabolic molecules in human epithelial cells. Top right: magnification of the cell in the center; scale: 120 nm/block. (E) Normal breast cell with interior view on the top right; scale: 200 nm/block; blue: cell membranes; green: organelles; pink: nuclear membranes; purple: nucleoli. (F) Cancer breast cell with interior view on the bottom right; scale: 200 nm/block.

walking through a ribosome-free version of the cell in Minecraft is shown in Video S2. The experimental setup included 1,950 ribosomes, representing 1% of the typical ribosomal count, which averages 195,000, as reported in previous studies (35, 36). This reduction in density helps students explore the inner structures without being frequently blocked by ribosomes. Additionally, the ribosomes were modeled as one 28-nm block, reflecting the typical 28–30-nm diameter of the ribosomes (37). Because of their irregular shape, the endoplasmic reticulum and Golgi apparatus cannot be extrapolated and displayed in this representation.

The minimal cell JCVI-syn3A provides an environment to experience a cell at a near-molecular resolution (Fig 5C). Unlike eukaryotic cells such as yeast, bacteria generally do not organize their insides into compartments. Rather than organelles such as mitochondria and nuclei, everything is mixed in a single compartment confined by a membrane in the Syn3A structure. The original WCM of Syn3A was constructed at 8-nm resolution, but the cytoplasm was too crowded for a user to explore at this resolution (5). To have the cytoplasm more open to explore and keep the original resolution of the chromosome model, each 8-nm block of the membrane and ribosomes

are represented by a $2 \times 2 \times 2$ set of 4-nm blocks. Each 4-nm block of DNA represents 12 bp of DNA, and the 543-kbp chromosome corresponds to a total of 46,188 blocks. The membrane of this Syn3A structure is 400 nm in diameter. For perspective, each mitochondrion in the yeast cell shown in Figure 5A is ~ 700 -nm long and 300-nm wide; ribosomes are roughly 20 nm in diameter. In the Syn3A structure, because each ribosome is larger than a single block, the ribosomes are represented as 3D cross shapes.

B. Breast cancer cells and normal breast cells

The Minecraft models generated from holotomographic images of human breast cells offer a unique perspective on the spatial features of cell biology. Because each block in this model is 200 nm across, the Minecraft player can enter the cell and observe from within. An expansive cell membrane made from blue-stained glass, heterogeneously shaped green concrete organelles, and huge pink-stained glass nuclear membranes surrounding purple concrete nucleoli can be observed. By initial inspection of the MDA-MB-231 cells in Minecraft (Figure 5F), we observed a spindle-shape morphology that is characteristic of metastatic cancer cells (38). The elongated shape and the increase in filopodia enable the cancer to invade healthy tissue. On the other hand, the hTERT-HME1 normal breast epithelial cells (Figure 5E) were observed to have a triangular or polygonal morphology, which is typical for normal epithelial cells. Using the segmented volumes of four MDA-MB-231 cells and four hTERT-HME1 cells, we quantified volumes of each feature and found that the cytoplasm, nuclei, and nucleoli were larger in the cancer cells than in the normal cells. The nucleus-to-cytoplasm volume ratio was 0.089 for the MDA-MB-231 cells and 0.098 for the hTERT-HME1 noncancer cells. The larger cytoplasm, nuclei, and nucleoli in the MDA-MB-231 cancer cells and the small difference in the nucleus-to-cytoplasm ratio are consistent with the morphological observations on the same cell lines seen in (15).

C. Metabolic molecules in epithelial cells

The spatial heterogeneity of the intracellular environment does not end at cell ultrastructure; that is, the chemical composition of the cell is spatially heterogeneous. For example, the DNA macromolecules are localized to the nucleus and mitochondria in eukaryotic cells, lipids are localized to membranes, and even the potential for chemical gradients of small molecules within the cell is possible. As an example of chemical heterogeneity imaging, we have converted a 2D image found in figure 5D in (10). The $1,550$ and $1,660 \text{ cm}^{-1}$ bands are commonly referenced for amide-rich materials (proteins). The 990 cm^{-1} band is potentially related to lipid and nucleic acid molecules. Because the image is a composite of these three channels, regions that are white indicate that all the IR bands composing the image have a strong signal in the corresponding pixels.

Although a 2D image cannot be explored in the same way as the 3D cell structures, it has provided useful insight for future structures collected by using similar methods. Incorporating the NDIR image emphasized the issue of color availability in Minecraft blocks. Segmented data such as the yeast model or holotomography imaging limit themselves to several colors dependent on the number of individually segmented structures. In the NDIR imaging, the color scheme is a continuum because each pixel has its own chemical identity in composition and concentrations. Additionally, this image illuminated the issue of cell size, image resolution, and field of view in Minecraft. The original image was collected at 30-nm resolution. At this resolution, the image could not be seen in a single field of view because of the size of human cells, so we reduced the image size from 988×988 to 247×247 pixels. An entire human cell is too large to be seen in an entire field of view, and future 3D structures can be constructed at multiple resolutions where low-resolution structures are used for entire cell perspectives and high-resolution structures allow players to explore the intracellular structures.

D. Accessibility of the Minecraft cell worlds

To have the Minecraft structures in this study accessible, we created a GitHub repository that has been organized to suit users of various education levels (20). The main folders include Worlds, Schematics, SchemGen_GUI, and Resources. For users who want to download only a Minecraft world containing a cell, they can navigate to the Worlds folder to directly download the Minecraft world files. This process is as easy as downloading a .zip file, unzipping it, and then dragging and dropping the unzipped folder into the Minecraft Saves folder on a computer with Minecraft installed. Video S1 is a visual guide of the process of downloading the world file for the minimal cell. More advanced users can access the schematic files to load cells into Minecraft through SchemGen_GUI and Schematics folders. The most advanced users can navigate to Resources to see the codes and programs used to generate the schematic files from experimental and computational data.

V. DISCUSSION

Using Minecraft, we can demonstrate the ultrastructure of cells from real experimental data. With yeast, we show that the detailed structure of each organelle and nucleus envelope can be shown. The cube size is 28 nm, which enables us to see the nuclear pore complexes. Further, we can compare the yeast with other prokaryotic cells, such as minimal cell syn3A. With this comparison, we clearly show that eukaryotic cells such as yeast have one vacuole, around three mitochondria, an endoplasmic reticulum, and a nucleus envelope, which prokaryotic cells do not have.

The Minecraft models are potential educational tools to show the differences between prokaryotic and eukaryotic cells. Furthermore, by comparing normal cells with cancer cells in Minecraft, the relevant morphological distinction related to cancer cells can be demonstrated. From label-free holotomography imaging and segmentation, we found quantitative differences that were

consistent with previous results. The Minecraft models also facilitate qualitative observations on the volume, shape, and distribution of cell features, highlighting structural differences between the normal and cancer cells.

Further, the model can be used to demonstrate the spatial distribution of proteins of interest and the process of targeted drug delivery. We could demonstrate how chemotherapeutic drugs induce the termination of cancer cells, providing an illustrative tool for cancer patients to understand how cancer treatment works.

Because our methods have separate modules and experimental data can be downloaded from an open-source database, educators may choose a pure course demonstration or a lab-coding hybrid mode that students can implement by using their own experimental data. For elementary school students or the general public, we highly recommend preparing the Minecraft world in advance and demonstrating and explaining the results in Minecraft. For middle and high school teachers, teachers can choose a hybrid method in which students can easily use the results from their wide-field light microscopy. For researchers using advanced imaging techniques, the workflow is a good tool to help them distribute their discovery to their colleagues or other students.

Minecraft is a multiplayer game, but it is only multiplayer if an online server is maintained. Hosting and maintaining a server require time to moderate the users because online interactions with others can become unpleasant or inappropriate. Additionally, hosting a Minecraft server requires computer resources (e.g., purchasing a paid third-party server or hosting on a local computer, neither of which is feasible for this scope of work). For these reasons, we will not host a multiplayer server. Online options to set up free temporary servers are available, and these could be used by small groups or classrooms to remove unwanted public exposure and still allow for multiplayer capabilities. Specific sites are not recommended here because there is no guarantee how long the individual third-party sites will be maintained.

VI. CONCLUSIONS

We have developed a comprehensive educational program comprising three modules designed for students with an interest in cellular structures. This program facilitates the learning of subcellular architectures, fundamental imaging techniques, and advanced topics, including image segmentation, image reconstruction, and computational methods for data extrapolation. By visualizing the structures of yeast and minimal cells in Minecraft, we conduct comparative analyses to highlight the distinctions between eukaryotic and bacterial cells. Additionally, this work showcases the application of our approach in the visualization of cancer and cancer-free cells, offering a novel educational tool to elucidate cancer subcellular structures. This program can be integrated into academic curricula and serves as an outreach tool to engage the general public. We anticipate that our initiative will spark increased interest in cellular biology among students and enhance public understanding of cancer mechanisms and treatments.

SUPPLEMENTAL MATERIAL

All programs, example Minecraft world files, and installation guide are available (20). Video S1: Demonstration of downloading and opening the Minimal Cell Minecraft cell world from (20). Video S2: Demonstration of walking through the yeast cell in Minecraft.

Supplemental files for this article are available at: <https://doi.org/10.35459/tbp.2024.000275.S1>.

AUTHOR CONTRIBUTIONS

TW, ZRT, KT, and ZL-S drafted and revised the manuscript. ZRT and ZL-S initiated the project. TW designed the teaching curriculum and built the workflow for the yeast. ZRT built the workflow for the minimal cell. KT built the workflow for the human breast cells and provided the segmentation script. SK, ZRT, and TW built the workflow for metabolites in human epithelial cells. TW wrote the code for the Minecraft Import GUI and prepared the GitHub repository. SAB, RB, and ZL-S provided project supervision. All authors reviewed and edited the manuscript.

ACKNOWLEDGMENTS

The authors were supported by or affiliated with the National Science Foundation's Science and Technology Center for Quantitative Cell Biology (NSF DBI-2243257). TW, ZRT, and ZL-S were supported in part by NSF MCB-2221237. This research was supported in part by a grant from the National Institutes of Health and the NIH/NIBIB P41 Center for Label-free Imaging and Multiscale Biophotonics (CLIMB) (1P41EB031772, S.A.B.; KT, SB, RB). We thank the Tumor Engineering and Phenotyping Shared Resource for graciously providing the hTERT-HME1 cell line (SK,

RB). This research was supported in part by NSF CBET 2229986 and NIH R01EB009745 (ZRT). Research reported in this publication was supported by the Cancer Center at Illinois–Beckman Institute Postdoctoral Fellows Program sponsored by the Cancer Center at Illinois and the Beckman Institute for Advanced Science and Technology, University of Illinois Urbana–Champaign (ZRT). The content is solely the responsibility of the authors and does not necessarily represent the official views of the program sponsors. The authors declare no competing interests.

REFERENCES

- Sontag, E. M., F. Morales-Polanco, J.-H. Chen, G. McDermott, P. T. Dolan, D. Gestaut, M. A. Le Gros, C. Larabell, and J. Frydman. 2023. Nuclear and cytoplasmic spatial protein quality control is coordinated by nuclear–vacuolar junctions and perinuclear ESCRT. *Nat Cell Biol* 25:699–713. <https://doi.org/10.1038/s41556-023-01128-6>.
- Nogales, E., and J. Mahamid. 2024. Bridging structural and cell biology with cryo-electron microscopy. *Nature* 628:47–56. <https://doi.org/10.1038/s41586-024-07198-2>.
- Xu, C. S., K. J. Hayworth, Z. Lu, P. Grob, A. M. Hassan, J. G. García-Cerdán, K. K. Niyogi, E. Nogales, R. J. Weinberg, and H. F. Hess. 2017. Enhanced FIB-SEM systems for large-volume 3D imaging. *eLife* 6: e25916. <https://doi.org/10.7554/eLife.25916>.
- Luthey-Schulten, Z. 2021. Integrating experiments, theory and simulations into whole-cell models. *Nat Methods* 18:446–447. <https://doi.org/10.1038/s41592-021-01150-2>.
- Thornburg, Z. R., D. M. Bianchi, T. A. Brier, B. R. Gilbert, T. M. Earnest, M. C. R. Melo, N. Safronova, J. P. Sáenz, A. T. Cook, K. S. Wise, C. A. Hutchison, H. O. Smith, J. I. Glass, and Z. Luthey-Schulten. 2022. Fundamental behaviors emerge from simulations of a living minimal cell. *Cell* 185:345–360.e28. <https://doi.org/10.1016/j.cell.2021.12.025>.
- Alawajee, O., and J. Delafield-Butt. 2021. Minecraft in education benefits learning and social engagement. *Int J Game-Based Learn* 11:19–56. <https://doi.org/10.4018/IJGBL.2021100102>.
- XBOX Game Studio Mojang Studios. 2011. Accessed 4 December 2024. <https://www.minecraft.net/en-us/>.
- Earnest, T. M., R. Watanabe, J. E. Stone, J. Mahamid, W. Baumeister, E. Villa, and Z. Luthey-Schulten. 2017. Challenges of integrating stochastic dynamics and cryo-electron tomograms in whole-cell simulations. *J Phys Chem B*, 121:3871–3881. <https://doi.org/10.1021/acs.jpcc.7b00672>.
- Cotte, Y., F. Toy, P. Jourdain, N. Pavillon, D. Boss, P. Magistretti, P. Marquet, and C. Depeursing. 2013. Marker-free phase nanoscopy. *Nat Photonics* 7:113–117. <https://doi.org/10.1038/nphoton.2012.329>.
- Kenkel, S., M. Gryka, L. Chen, M. P. Confer, A. Rao, S. Robinson, K. V. Prasanth, and R. Bhargava. 2022. Chemical imaging of cellular ultrastructure by null-deflection infrared spectroscopic measurements. *Proc Natl Acad Sci U S A* 119:e2210516119. <https://doi.org/10.1073/pnas.2210516119>.
- Breuer, M., T. M. Earnest, C. Merryman, K. S. Wise, L. Sun, M. R. Lynott, C. A. Hutchison, H. O. Smith, J. D. Lapek, D. J. Gonzalez, V. de Crécy-Lagard, D. Haas, A. D. Hanson, P. Labhsetwar, J. I. Glass, and Z. Luthey-Schulten. 2019. Essential metabolism for a minimal cell. *eLife* 8:e36842. <https://doi.org/10.7554/elife.36842>.
- Hinnebusch, A. G., and M. Johnston. 2011. YeastBook: an encyclopedia of the reference eukaryotic cell. *Genetics* 189:683–684. <https://doi.org/10.1534/genetics.111.135129>.
- Buser, C. 2010. Toward sub-second correlative light and electron microscopy of *Saccharomyces cerevisiae*. *Methods Cell Biol* 96:217–234. [https://doi.org/10.1016/S0091-679X\(10\)96010-X](https://doi.org/10.1016/S0091-679X(10)96010-X).
- U.S. Centers for Disease Control and Prevention, U.S. Cancer Statistics. 2023. United States cancer statistics: data visualizations. Accessed 1 March 2024. <https://www.cdc.gov/cancer/dataviz>.
- Nandakumar, V., L. Kelbauskas, K. F. Hernandez, K. M. Lintecum, P. Senechal, K. J. Bussey, P. C. W. Davies, R. H. Johnson, and D. R.

- Meldrum. 2012. Isotropic 3D nuclear morphometry of normal, fibro-cystic and malignant breast epithelial cells reveals new structural alterations. *PLoS One* 7:e29230. <https://doi.org/10.1371/journal.pone.0029230>.
16. McNally, D. L., L. J. MacDougall, B. E. Kirkpatrick, C. V. Maduka, T. E. Hoffman, B. D. Fairbanks, C. N. Bowman, S. L. Spencer, and K. S. Anseth. 2023. Reversible intracellular gelation of mcf10a cells enables programmable control over 3D spheroid growth. *Adv Healthcare Mater* 13:2302528. <https://doi.org/10.1002/adhm.202302528>.
 17. Gan, L., and G. J. Jensen. 2012. Electron tomography of cells. *Quart Rev Biophys* 45:27–56. <https://doi.org/10.1017/S0033583511000102>.
 18. Turk, M., and W. Baumeister. 2020. The promise and the challenges of cryo-electron tomography. *FEBS Lett* 594:3243–3261. <https://doi.org/10.1002/1873-3468.13948>.
 19. Cuhe, E., P. Marquet, and C. Depeursinge. 1999. Simultaneous amplitude-contrast and quantitative phase-contrast microscopy by numerical reconstruction of Fresnel off-axis holograms. *Appl Opt* 38:6994–7001. <https://doi.org/10.1364/AO.38.006994>.
 20. Wu, T., Z. R. Thornburg, K. Tan, S. Kenkel, S. A. Boppart, R. Bhargava, and Z. Luthey-Schulten. GitHub: Luthey-Schulten-Lab. 2024. Accessed 4 December 2024. <https://github.com/Luthey-Schulten-Lab/CraftCells>.
 21. Iudin, A., P. K. Korir, S. Somasundharam, S. Weyand, C. Cattavittello, N. Fonseca, O. Salih, G. J. Kleywegt, and A. Patwardhan. 2023. EMPIAR: the Electron Microscopy Public Image Archive. *Nucleic Acids Res* 51:D1503–D1511. <https://doi.org/10.1093/nar/gkac1062>.
 22. The wwPDB Consortium, J. Turner, S. Abbott, N. Fonseca, R. Pye, L. Carrijo, A. Kumari Duraisamy, O. Salih, Z. Wang, G. J. Kleywegt, K. L. Morris, A. Patwardhan, S. K. Burley, G. Crichlow, Z. Feng, J. W. Flatt, S. Ghosh, B. P. Hudson, C. L. Lawson, Y. Liang, E. Peisach, I. Persikova, M. Sekharan, C. Shao, J. Young, S. Velankar, D. Armstrong, M. Bage, W. Morellato Bueno, G. Evans, R. Gaborova, S. Ganguly, D. Gupta, D. Harrus, A. Tanweer, M. Bansal, V. Rangannan, G. Kurisu, H. Cho, Y. Ikegawa, Y. Kengaku, J. Y. Kim, S. Niwa, J. Sato, A. Takuwa, J. Yu, J. C. Hoch, K. Baskaran, W. Xu, W. Zhang, and X. Ma. 2024. EMDb—the Electron Microscopy Data Bank. *Nucleic Acids Res* 52: D456–D465. <https://doi.org/10.1093/nar/gkad1019>.
 23. Shan Xu, C., S. Pang, G. Shtengel, A. Müller, A. T. Ritter, Hu. K. Hoffman, S.-y. Takemura, Z. Lu, H. A. Pasolli, N. Iyer, J. Chung, D. Bennett, A. V. Weigel, M. Freeman, S. B. Van Engelenburg, T. C. Walther, R. V. Farese, J. Lippincott-Schwartz, I. Mellman, M. Solimena, and H. F. Hess. 2021. An open-access volume electron microscopy atlas of whole cells and tissues. *Nature* 599:147–151. <https://doi.org/10.1038/s41586-021-03992-4>.
 24. Kremer, J. R., D. N. Mastronarde, and J. R. McIntosh. 1996. Computer visualization of three-dimensional image data using IMOD. *J Struct Biol* 116:71–76. <https://doi.org/10.1006/j.sbi.1996.0013>.
 25. Tang, G., L. Peng, P. R. Baldwin, D. S. Mann, W. Jiang, I. Rees, and S. J. Ludtke. 2007. EMAN2: an extensible image processing suite for electron microscopy. *J Struct Biol* 157:38–46. <https://doi.org/10.1016/j.jsb.2006.05.009>.
 26. Martinez-Sanchez, A., I. Garcia, S. Asano, V. Lucic, and J.-J. Fernandez. 2014. Robust membrane detection based on tensor voting for electron tomography. *J Struct Biol* 186:49–61. <https://doi.org/10.1016/j.jsb.2014.02.015>.
 27. Harris, C. R., K. J. Millman, S. J. van der Walt, R. Gommers, P. Virtanen, D. Cournapeau, E. Wieser, J. Taylor, S. Berg, N. J. Smith, R. Kern, M. Picus, S. Hoyer, M. H. van Kerkwijk, M. Brett, A. Haldane, J. Fernández del Río, M. Wiebe, P. Peterson, P. Gérard-Marchant, K. Sheppard, T. Reddy, W. Weckesser, H. Abbasi, C. Gohlke, and T. E. Oliphant. 2020. Array programming with NumPy. *Nature* 585:357–362. <https://doi.org/10.1038/s41586-020-2649-2>.
 28. Virtanen, P., R. Gommers, T. E. Oliphant, M. Haberland, T. Reddy, D. Cournapeau, E. Burovski, P. Peterson, W. Weckesser, J. Bright, S. J. van der Walt, M. Brett, J. Wilson, K. J. Millman, N. Mayorov, A. R. J. Nelson, E. Jones, R. Kern, E. Larson, C. J. Carey, Í. Polat, Y. Feng, E. W. Moore, J. VanderPlas, D. Laxalde, J. Perktold, R. Cimman, I. Henriksen, E. A. Quintero, C. R. Harris, A. M. Archibald, A. H. Ribeiro, F. Pedregosa, P. van Mulbregt, and SciPy 1.0 Contributors. 2020. SciPy 1.0: fundamental algorithms for scientific computing in Python. *Nat Methods*, 17:261–272. <https://doi.org/10.1038/s41592-019-0686-2>.
 29. Gilbert, B. R., Z. R. Thornburg, V. Lam, F.-Z. M. Rashid, J. I. Glass, E. Villa, R. T. Dame, and Z. Luthey-Schulten. 2021. Generating chromosome geometries in a minimal cell from cryo-electron tomograms and chromosome conformation capture maps. *Front Mol Biosci* 8:644133. <https://doi.org/10.3389/fmolb.2021.644133>.
 30. C. T. Rueden, J. Schindelin, M. C. Hiner, B. E. DeZonia, A. E. Walter, E. T. Arena, and K. W. Eliceiri. 2017. ImageJ2: ImageJ for the next generation of scientific image data. *BMC Bioinformatics* 18:529. <https://doi.org/10.1186/s12859-017-1934-z>.
 31. Rueden, C. T., M. C. Hiner, E. L. Evans, M. A. Pinkert, A. M. Lucas, A. E. Carpenter, B. A. Cimini, and K. W. Eliceiri. 2022. PyImageJ: a library for integrating ImageJ and Python. *Nat Methods* 19:1326–1327. <https://doi.org/10.1038/s41592-022-01655-4>.
 32. Li, C. H., and C. K. Lee. 1993. Minimum cross entropy thresholding. *Pattern Recognit* 26:617–625. [https://doi.org/10.1016/0031-3203\(93\)90115-D](https://doi.org/10.1016/0031-3203(93)90115-D).
 33. Legland, D., I. Arganda-Carreras, and P. Andrey. 2016. MorphoLibJ: integrated library and plugins for mathematical morphology with ImageJ. *Bioinformatics* 32:3532–3534. <https://doi.org/10.1093/bioinformatics/btw413>.
 34. Ollion, J., J. Cochenec, F. Loll, C. Escudé, and T. Boudier. 2013. TANGO: a generic tool for high-throughput 3D image analysis for studying nuclear organization. *Bioinformatics* 29:1840–1841. <https://doi.org/10.1093/bioinformatics/btt276>.
 35. Kumar Biswas, S., M. Yamaguchi, N. Naoe, T. Takashima, and K. Takeo. 2003. Quantitative three-dimensional structural analysis of *Exophiala dermatitidis* yeast cells by freeze-substitution and serial ultrathin sectioning. *J Electron Microsc (Tokyo)* 52:133–143. <https://doi.org/10.1093/jmicro/52.2.133>.
 36. Yamaguchi, M., Y. Namiki, H. Okada, Y. Mori, H. Furukawa, J. Wang, M. Ohkusu, and S. Kawamoto. 2011. Structome of *Saccharomyces cerevisiae* determined by freeze-substitution and serial ultrathin-sectioning electron microscopy. *J Electron Microsc (Tokyo)* 60:321–335. <https://doi.org/10.1093/jmicro/dfr052>.
 37. Cox, R. A., and H. R. V. Arnstein. 2003. Translation of RNA to protein. In *Encyclopedia of Physical Science and Technology*. 3rd ed. Academic Press, pp. 31–51. <https://doi.org/10.1016/B0-12-227410-5/00788-2>.
 38. Sun, J., H. He, Y. Xiong, S. Lu, J. Shen, A. Cheng, W.-C. Chang, M.-F. Hou, J. M. Lancaster, M. Kim, and S. Yang. 2011. Fascin protein is critical for transforming growth factor β protein-induced invasion and filopodia formation in spindle-shaped tumor cells. *J Biol Chem* 286:38865–38875. <https://doi.org/10.1074/jbc.M111.270413>.